ELSEVIER

International Journal of Mass Spectrometry 218 (2002) 265–279

International Journal of Mass Spectrometry

www.elsevier.com/locate/ijms

Higher-resolution data-dependent selective external ion accumulation for capillary LC-FTICR

Mikhail E. Belov, Gordon A. Anderson, Richard D. Smith*

Environmental Molecular Sciences Laboratory, Pacific Northwest National Laboratory, P.O. Box 999, MS: K8-98, Richland, WA 99352, USA

Received 10 April 2002; accepted 29 May 2002

Abstract

Data-dependent selective external ion ejection with improved resolution is demonstrated with a 3.5 T Fourier transform ion cyclotron resonance (FTICR) instrument employing dynamic range enhancement applied to mass spectrometry (DREAMS) technology. To correct for the fringing rf-field aberrations each rod of the selection quadrupole has been segmented into three sections, so that ion excitation and ejection was performed by applying auxiliary rf-only waveforms in the region of the middle segments. Two different modes of external ion trapping and ejection were studied with the mixtures of model peptides and a tryptic digest of bovine serum albumin (BSA). A mass resolution of about 100 has been attained for rf-only dipolar ejection in a quadrupole operating at a Mathieu parameter (q) of ~0.45. LC-ESI-DREAMS-FTICR analysis of a 0.1 mg/mL solution of BSA digest resulted in detection of 82 unique tryptic peptides with mass measurement errors lower than 5 ppm, providing 100% sequence coverage of the protein. (Int J Mass Spectrom 218 (2002) 265–279)

1. Introduction

Capillary liquid chromatography/mass spectrometry (LC/MS) has become a powerful analytical method in many areas of biological research [1–6]. One of the most challenging applications of LC/MS in the "post-genomic era" is the analysis of the complex arrays of proteins (i.e., proteome) expressed by an organism, cell culture or tissue in an attempt to unravel complex cellular pathways under various physiological conditions [7–13]. When coupled to an LC separation [14], Fourier transform ion cyclotron resonance (FTICR) mass spectrometry [15,16] has been shown to be an ultra-sensitive, high mass measurement accuracy approach for characterization of proteolytic digests [17–20]. The sensitivity provided by FTICR has been shown to be increased by ion trapping and accumulation in a 2D rf-only octopole trap positioned externally to an FTICR mass spectrometer [21]. The usefulness of ion pre-selection with FTICR was originally recognized by Mciver [22], who proposed using a quadrupole ion guide operating at an elevated pressure. This quadrupole could be used for the quadrupole mass filtering (rf/dc) of ions generated by an external ion source. The ions could then be trapped in the FTICR cell using conventional gas-assisted accumulated trapping [23]. Wang et al. [24] have recently demonstrated low-resolution external mass-selective ion accumulation with a 2D octopole ion trap. The development of selective external ion accumulation [17,25] when most abundant ion species can be selectively ejected using either quadrupole mass filtering

* Corresponding author. E-mail: rd_smith@pnl.gov

1387-3806/02/$ – see front matter
PII S1387-3806(02)00736-4

or rf-only resonant dipolar excitation [26–28] prior to ion accumulation enhanced the sensitivity of FTICR measurements by two orders of magnitude.

We have recently reported on a dynamic range enhancement applied to mass spectrometry (DREAMS) technology that provides, e.g., greatly enhanced characterization of peptides in the course of a capillary LC separation of proteomic digests [29]. This approach requires detection of a mass spectrum acquired during the non-selective accumulation, software-controlled selection of the *m*/*z*'s of the most abundant ion peaks based on their quadrupole secular frequencies followed by selective rf-only ejection of the most abundant species prior to external accumulation in the next scan immediately following the non-selective accumulation. Removal of these major species and the following accumulation for extended periods of lower abundance species result in an increase in the dynamic range. Though a 40% increase in the number of identified putative peptides resulting from a tryptic digest of a yeast proteome has been achieved as compared to that of the conventional non-selective ion accumulation, there is a significant room for improvement and refinement of the DREAMS approach related to (1) optimizing the number and intensities of ions selected, (2) optimizing the accumulation times for both the initial (non-selective) and second (selective) ion accumulations, and, of particular focus of this work, (3) increasing the resolution of ion ejection. Lower-resolution ion pre-selection prior to external ion accumulation in a multipole ion trap gives rise to the appearance of small "notches" in a mass spectrum, centering on the ejected high abundant ion species. Lower abundance peptide species dispersed in the mass spectrum within these "notches" would be irrevocably ejected from the multipole ion trap. Therefore, increasing the mass resolution of the DREAMS ion pre-selection is important for increasing the number of detected peptides in the course of a capillary LC separation and for increasing the overall dynamic range of proteomic measurements.

Cha et al. [30] have shown that, by using lower-amplitude rf-only dipolar excitation, ion species of reserpine ions stored for 100 ms in a 2D quadrupole ion trap ($q = 0.7$) can be efficiently ejected with a mass resolution of 250. An important parameter for achieving this mass resolution was found to be the parameter Mathieu (q) defined as follows [31]:

$$q = \frac{4zeV_{\mathrm{rf}}}{m\omega_0^2 r_0^2} \tag{1}$$

where V_{rf} is the peak-to-ground rf-amplitude, z the ion charge state, e the elementary charge, m the ion mass, ω_0 the rf-field angular frequency, and r_0 is the quadrupole inscribed radius.

Mass resolution for ion ejection was found to reduce to 68 with a decrease in q to 0.3. It is important to realize that since q is an m/z-dependent parameter, the resonant ejection of peaks at the higher m/z end of a mass spectrum (at $q \sim 0.7$) will result in undesired ion instability of lower m/z ion species and their biased representation in acquired mass spectra.

Increasing the space charge in the selection quadrupole results in ion–ion interactions, giving rise to a decrease in the secular frequency and an increase in the threshold amplitude of an auxiliary rf-field accompanied by the loss of selectivity and resolution during ion ejection [25,29]. In addition, the increased space charge distorts harmonic distribution of the quadrupole pseudo-potential [32], resulting in off-resonant excitation at larger radii. Therefore, rather than being ejected from the quadrupole, ions excited to larger radii will experience beat oscillations, gain additional kinetic energy from the rf-field, and more likely dissociate due to collisions with the background gas [29].

Another perturbation to ion motion in 2D quadrupole ion traps is caused by the fringing rf-fields. The fringing rf-field effect on the resolution of a quadrupole mass filter has been studied in earlier works by Brubaker [33], Dawson [34] and Fite [35]. Additional electrodes with only rf-potential applied were used to correct for the fringing rf-fields at the quadrupole entrance [33,34]. A leaky dielectric tube, which shields against dc and low-frequency ac-fields while not shielding against rf-fields, was placed at the entrance of a quadrupole mass filter, providing a delayed dc-ramp characterized by increased mass resolution

[35]. Ion trapping in a 2D rf-only quadrupole imposes additional constraints. If ions are axially trapped between two plates supplied only with dc-potentials, the *m*/*z*-dependent axial component of the fringing rf-field results in spatial separation of different *m*/*z* species decelerating in the fringing field. In order to minimize fringing field-induced *m*/*z* discrimination, the dc-potentials applied to the trapping plates need to be increased [36]. This increase in the trapping dc-potentials is accompanied by an increase in the radial component of the dc-field, causing ion deflection to larger radii, where they can gain additional kinetic energy from the rf-field, again resulting in undesired fragmentation due to collisions with neutral molecules.

In this work we report on the improved design for the selection quadrupole that enabled us to achieve a mass resolution for resonant ion ejection of ∼100 at $q \sim 0.4$ and higher space charge. Higher-resolution ion pre-selection was performed with a capillary LC separation of a bovine serum albumin (BSA) digest followed by the DREAMS approach implemented with a 3.5 T FTICR instrument.

2. Experimental

2.1. Instrument

The FTICR mass spectrometer used in the present studies is based on a 3.5 T unshielded solenoid magnet (Oxford Instruments, UK) and a vacuum system design previously described [17]. The mass spectrometer incorporates the ESI ion source with an electrodynamic ion funnel [37] and a quadrupole for collisional focusing, an external accumulation interface [17,25], an electrostatic ion guide and an FTICR cylindrical dual cell combination. An Odyssey data station (Finnigan Corp., San Jose, CA) controlled the timing and potential distribution during the experiment. To implement data-dependent selective external ion accumulation, a 12-bit ADC (National Instruments, Austin, TX) coupled to a Pentium PC running our ICR-2LS software was utilized for parallel data acquisition.

Fig. 1 shows the external accumulation interface comprising three quadrupoles, which will further be referred to as “ion guiding,” “selection” and “accumulation” quadrupoles. Compared to the earlier reported design [17], each rod of the 100 mm long selection quadrupole was segmented into three parts, so that 50 mm long middle segments separated 25 mm long end segments. Resonant rf-only dipolar excitation was used for ion ejection from the selection quadrupole [27,28]. To eliminate the effect of the fringing rf-field, auxiliary rf-excitation was applied to the middle segments of two opposite rods of the selection quadrupole coupled to the secondary coil of a 1:1 transformer. The middle point of the transformer secondary coil was driven by the main rf-drive at amplitudes of 300–600 $V_{p–p}$ and frequencies ranging from 500 to 700 kHz. Excitation waveforms generated by the PC were then applied to the primary coil of the transformer.

2.2. Data-dependent acquisition

The DREAMS approach was implemented with two alternating sequences [29]. Ions generated by the ESI source were non-selectively trapped in the accumulation quadrupole. Following a short storage period the externally accumulated ions were ejected to the FTICR cell and captured using gated trapping [38–40]. During the storage period used for collisional damping of the ion’s kinetic energy in the accumulation quadrupole, the rf-potential on the collisional quadrupole rods was switched off so that no ions from the ESI could enter the accumulation region. During ion excitation in the FTICR cell a trigger pulse was applied to the 12-bit ADC making it ready for data acquisition. Acquired mass spectra were converted to secular frequency spectra (of ion oscillation) in the selection quadrupole and a superposition of excitation sine waveforms synthesized with our ICR-2LS software (developed by G. Anderson and J. Bruce) was generated by a 32K plug-in PC DAC board (National Instruments, Austin, TX) and then applied to the middle segments of the selection quadrupole rods as an auxiliary rf-field. Using this approach one or several

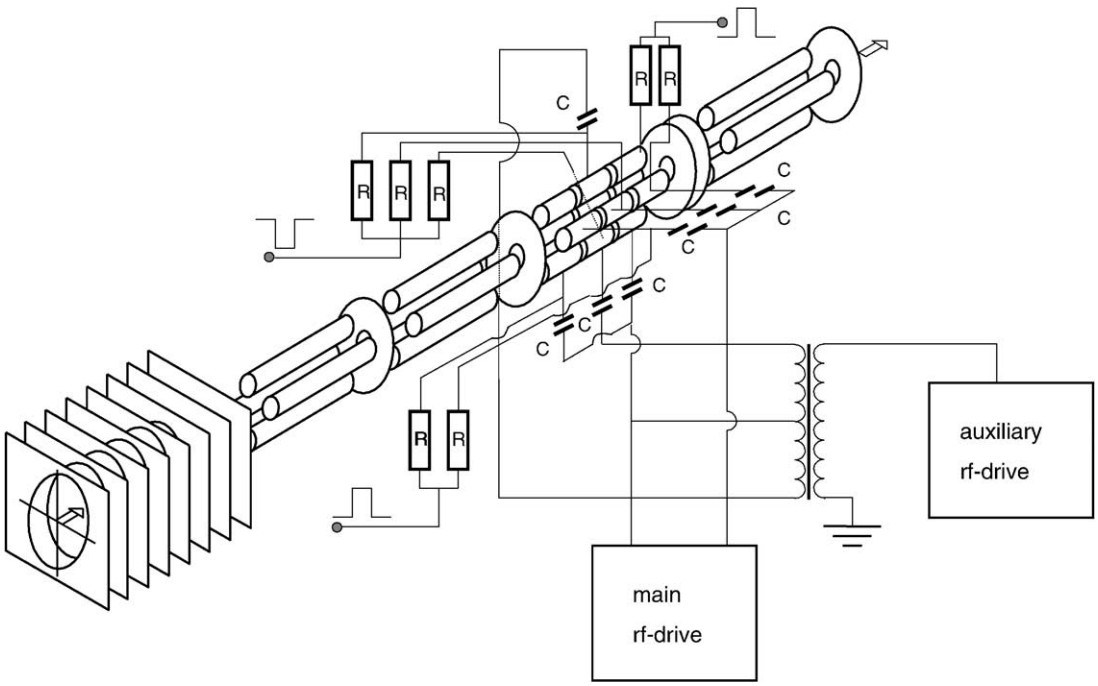

Fig. 1. A schematic of the interface for selective ion accumulation coupled to the ESI source. The ESI source elements: 1 is the ion funnel, 2 is the collisional quadrupole, 3 is the conductance limit between the ion guiding and the collisional quadrupoles. The elements of the interface: 4 is the ion guiding quadrupole, 5 is the entry plate of the selection quadrupole, 6 is the segmented selection quadrupole, 7 is the exit plate of the selection quadrupole, 8 is the entry plate of the accumulation quadrupole, 9 is the segmented accumulation quadrupole, 10 is the exit plate of the accumulation quadrupole. Auxiliary excitation waveforms are applied to the middle segments of the selection quadrupole. The end and middle segments of the selection quadrupole are independently driven using a multi-channel pulse-voltage generator, to create an axial potential well in the region of the middle segments. $R = 7.5\,\mathrm{k\Omega}$ (10 W), $C = 1\,\mathrm{nF}$.

of the most abundant species were ejected from the selection quadrupole, resulting in external ion accumulation of lower abundant species for extended periods. To maintain higher duty cycle, the auxiliary rf-field was switched off immediately following the ion transfer to the FTICR cell, thus allowing for the non-selective external ion trapping in the accumulation quadrupole while analyzing the lower abundant ion species in the FTICR cell.

2.3. Sample preparation

Peptides were purchased from Sigma (Sigma Chemicals, St. Loius, MO) and were used without further purification dissolved in a water:methanol:acetic acid solution (49:49:2 vol.%) at different concentrations ranging from 0.1 mg/mL to 2 pg/mL. The solutions were infused into the ESI source at a flow rate of 300 nL/min using a syringe pump (Harvard, South Natick, MA). HPLC/FTICR MS data sets were obtained using a commercial HPLC system (ISCO Inc., Lincoln, NE). The tryptic peptides were injected onto a 150 μm i.d. × 60 cm long capillary column packed with a 5 μm diameter C_{18} separation medium (POROS 20R2, Perspective Biosystem, Framingham, MA). A solvent gradient was used to elute the peptides using 0.4% acetic acid in water (solvent A) and 0.4% acetic acid in 80% acetonitrile (solvent B). The peptides were eluted using a linear gradient of 0–80% solvent B over 60 min. Solvents were delivered to the capillary column at a pressure of 6000 psi using two ISCO model 100 DM pumps controlled by an ISCO series D

controller and a LC Packings Accurate microflow processor splitter (LC Packings, San Francisco, CA) resulting in a capillary flow rate of 1 mL/min.

3. Results and discussion

Resonant ion ejection from the selection quadrupole was studied in two different modes. Fig. 2 shows the distributions of pulsed voltages applied to the selection quadrupole in the "trapping" mode. During the 5 ms trapping event the dc-potential applied to the entrance conductance limit (part 1 in Fig. 2) was tuned to match the mean kinetic energy of the incoming ion beam (typically ∼10 V) while the rear conductance limit (part 5) was maintained at a potential exceeding the kinetic energy of the fastest ions by a few volts (∼15 V). All the segments of the selection quadrupole were biased to 7 V. Increasing the length of a trapping volume (i.e., by trapping ions between the conductance limits rather than in the middle segment region) results in higher trapping efficiency due to a greater number of ion–neutral collisions across the selection quadrupole. Following trapping, the dc-potential applied to the middle segments of the selection quadrupole (part 3) was reduced by a few volts to create an axial potential well for a trapped ion cloud. Ion cloud trapped in the entire volume of the selection quadrupole would then redistribute due to Coulombic repulsion to occupy the middle segment region. The

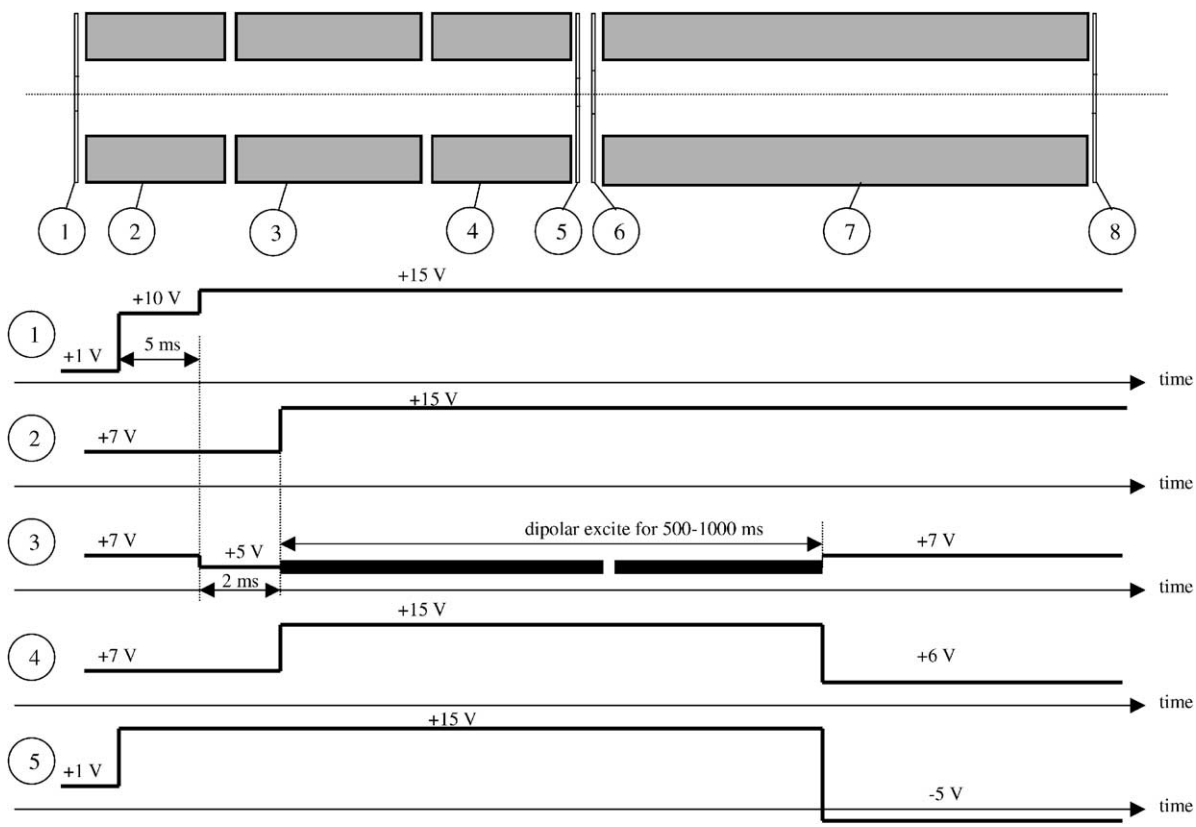

Fig. 2. Experimental steps used for trapping and selection of ions in the selection quadrupole ("trapping mode"). Ions accumulated for 5 ms between the selection quadrupole conductance limits were transferred for 2 ms to the region of the middle segments and selectively ejected for a variable period (∼500–1000 ms) employing resonant dipolar excitation. The ion species remaining in the selection quadrupole were then transferred to the ICR cell for subsequent gated trapping.

entrance conductance limit potential (part 1 in Fig. 2) was increased to ∼15 V, so that no ions from the ESI source could enter the selection quadrupole. After a short delay (∼1–2 ms) the dc-bias on the end segments (parts 2 and 4) was increased to match the potentials applied to the conductance limits, preventing ions from being trapped in the region of the end segments. Following the increase in the end segment potential, resonant dipolar excitation was applied to a pair of the middle segments to selectively eject particular *m*/*z* ion species. Such an excitation eliminates contribution of the fringing aberrations of the main rf-field to ion motion. To increase mass resolution for resonant ejection, dipolar excitation was performed at the lowest possible amplitude (i.e., threshold amplitude) and for extended periods (∼1 s). Ion excitation was followed by ion ejection from the selection quadrupole when potentials applied to the middle and exit segments (parts 3 and 4) were 7 and 6 V, respectively. The potentials on the entry and exit conductance limits, and the dc-bias of the accumulation quadrupole were 6, 5 and 1 V, respectively. The ejected ion cloud was then captured in the FTICR cell using gated trapping.

Fig. 3 shows distribution of the dc-potentials applied to the selection quadrupole in the "pseudo-trapping" mode. An axial potential well of a few volts was created in the middle segment region of the selection quadrupole (part 3 in Fig. 3) while keeping all the end segments and both conductance limits at the same potential (∼10 V). Since ions were continuously entering the selection quadrupole during an accumulation period (i.e., a time interval when an rf-potential was applied to the collision quadrupole rods), a steady-state ion population was trapped in the middle segment region, so that ions entering from the ESI source effectively pushed the trapped ions out of the selection quadrupole for subsequent trapping in the accumulation quadrupole. This "pseudo-trapping" increases the ion's residence time in the middle segment region and makes excitation conditions less dependent on space charge as compared to the "trapping" mode. Similar to the "trapping" mode, resonant dipolar excitation was applied to the middle segments of the selection quadrupole during the entire accumulation period. Following a 5 ms accumulation period, ions were stored for 100 ms in the accumulation quadrupole to damp their kinetic energy in collisions with the background gas and then ejected to the FTICR cell.

Fig. 4A shows a typical mass spectrum of a 10^{-6} M mixture of bradykinin, angiotensin I, substance P, and neurotensin obtained in the "trapping" mode. Ions injected into the selection quadrupole for 5 ms were trapped between the conductance limits. Following ion trapping, a 2 V deep axial potential well was created in the region of the middle segments, where ions were rapidly transferred (∼1 ms) and stored for 1 s. Auxiliary rf-excitation at a variable frequency and a peak-to-peak amplitude of 45 mV was applied to a pair of the middle segments to selectively eject ions from the quadrupole during the storage period. Selective ion ejection was then followed by ion transfer to the FTICR cell. Fig. 4B shows the dependence of $[Br + 2H]^{2+}$ ion intensity on the frequency of the exciting rf-field in the "trapping mode." The parameters of the main rf-field (a peak-to-peak amplitude of 300 V and a frequency of 600 kHz) corresponded to a *q* value of 0.45 for *m*/*z* 530.78. FWHM mass resolution for ion ejection was about 90, indicating a three-fold increase compared with our previously published results [17,25]. Interestingly, the dependence of $[Br + 2H]^{2+}$ ion intensity on the frequency of the exciting rf-field was found to be asymmetric, yielding higher resolution (∼150) when approaching the resonance from the higher frequency side (i.e., lower *m*/*z*). We attribute this asymmetry to the distortion of the quadrupole harmonic pseudo-potential in the close proximity of circular quadrupole rods, resulting in non-linear ion oscillations at larger radii. Space charge introduces additional non-linear effects [41]. It is well known from the theory of a non-linear oscillator experiencing external periodic excitation that dependence of the oscillator amplitude on the frequency of an external force is skewed due to the non-linear terms in the equation of motion [42–44]. When approaching the exact resonance from the higher frequency side, the oscillator amplitude exhibits an increase to a stable branch. This "jump" phenomenon has been invoked to explain high experimental mass resolution

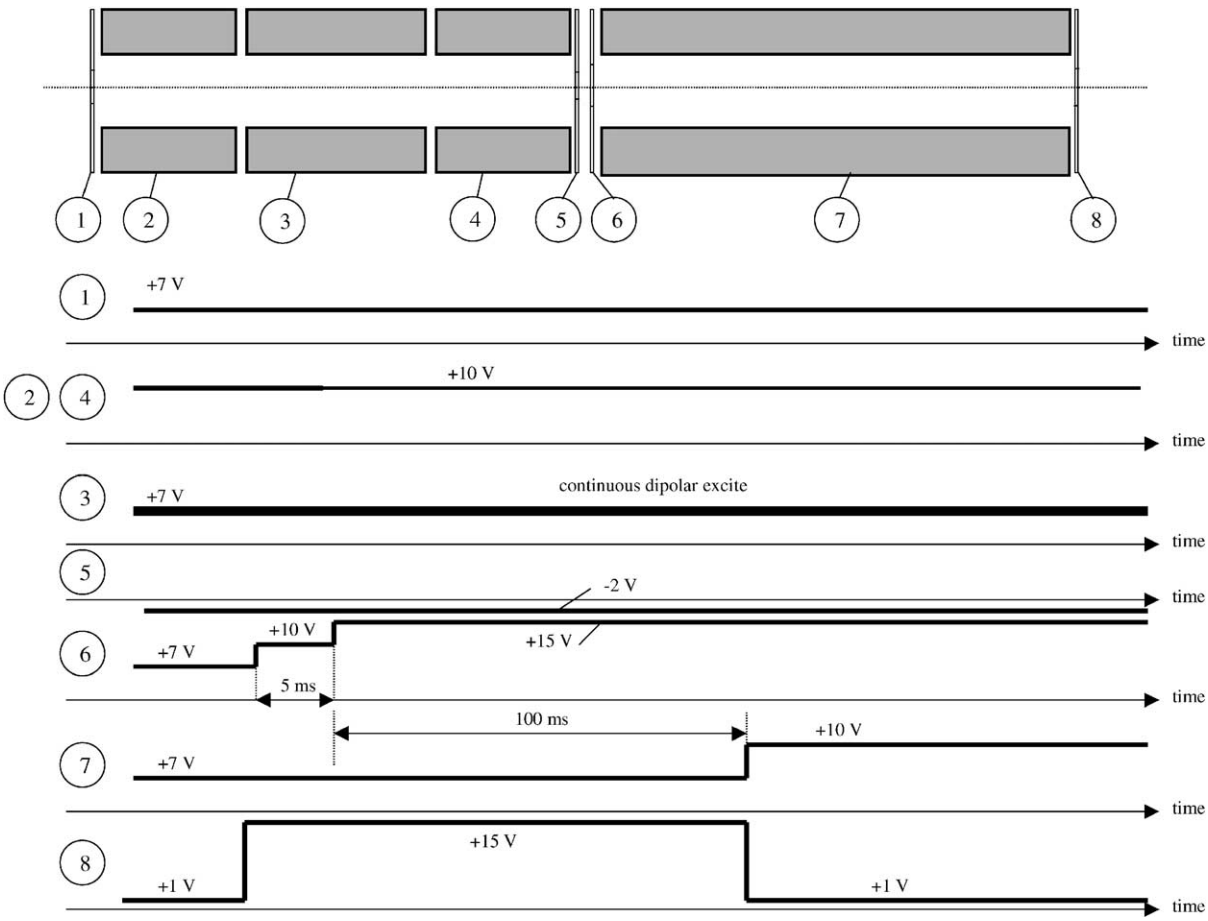

Fig. 3. Experimental steps used for ion ejection in the middle segment of the selection quadrupole followed by ion trapping in the accumulation quadrupole and gated trapping in the FTICR cell ("pseudo-trapping mode"). An axial potential well of 3 V was used for lower-efficiency ion trapping in the selection quadrupole accompanied by the selective ion ejection in the region of the middle segments. Ions traversing this axial potential well were trapped for 5 ms in the accumulation quadrupole and, following a 100 ms storage period, transferred to the FTICR cell for subsequent gated trapping and analysis.

and differences in mass resolution for ion ejection depending on the rate and direction of scanning for a stretched 3D quadrupole ion trap [45,46]. We believe that similar jump of the amplitude of ion oscillations occurs in a 2D rf-only quadrupole ion trap and it may account for higher resolution for ion ejection at frequencies just above the exact resonance.

Fig. 5A and B shows mass spectra of a 10^{-7} M solution of polyethylene glycol ($MW_{aver} = 1400$ Da) obtained in the "pseudo-trapping" mode. The mass spectrum in Fig. 5A was acquired using non-selective trapping in the accumulation quadrupole (A), while the mass spectrum in Fig. 5B was obtained employing selective ion ejection in the selection quadrupole prior to ion trapping in the accumulation quadrupole (B). The potential applied to the middle segments of the selection quadrupole was lower than that of the end segments by 2 V, thus creating an axial potential well in the region of the middle segments. Dipolar excitation sine waveforms applied to a pair of the middle segments at frequencies, corresponding to the doubled ion's secular frequencies (i.e., parametric excitation),

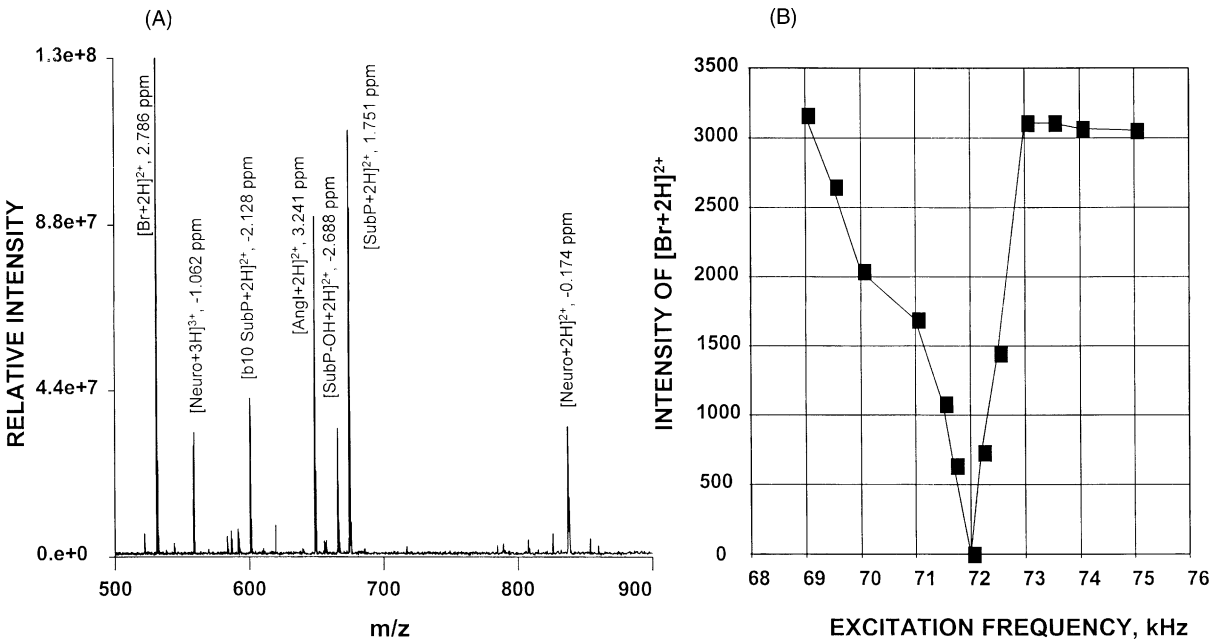

Fig. 4. (A) Typical mass spectrum of a 10^{-6} M mixture of bradykinin (Br), angiotensin I (AngI), substance P (SubP), and neurotensin (Neuro) obtained in the "trapping" mode. Mass measurement errors are shown for major identified peaks. (B) Intensity of the doubly charged bradykinin ion peak $[Br + 2H]^{2+}$ as a function of the frequency of auxiliary rf-excitation.

were used to eject selected species on the fly through the selection quadrupole. An axial potential well in the region of the middle segments resulted in ion deceleration and longer residence time in the selection quadrupole as compared to use of a conventional quadrupole of the same length. The inset to Fig. 5B shows the region of mass spectra affected by the use of 300 $mV_{p–p}$ auxiliary parametric rf-excitation at a frequency of 197 kHz. The mass resolution for ejection of polymer ions from the selection quadrupole (*m*/*z* 777.65, $q \sim 0.45$) was measured to be about 80. It should be noted that ejection of ions decelerating in the middle section of the selection quadrupole was found to be robust to variations in the incoming ion current. For example, we found that varying the entry currents to the selection quadrupole over two orders of magnitude (10 pA to 1 nA) results in ~20% variation in the resonant dipolar excitation frequency, in accord with earlier observations by Paul et al. [26]. This feature of the selective ion ejection in the "pseudo-trapping" mode makes it attractive for use in conjunction with DREAMS and LC separations of proteolytic digests.

Fig. 6A and B shows the total ion current (TIC) chromatograms and typical mass spectra of a 0.1 mg/mL solution of BSA acquired using the DREAMS approach (i.e., the alternating non-selective (A) and selective (B) accumulation scans). One the most abundant ion species identified in each non-selective accumulation scan was ejected from the selection quadrupole during the selective accumulation scan, which immediately followed. The procedure for calculating calibration coefficients to convert *m*/*z* spectra to secular frequency spectra of ion oscillations in the selection quadrupole has been described in detail elsewhere [29]. Ion ejection was performed in the "pseudo-trapping" mode at the secular frequency of the excited ion species. The BSA tryptic fragments identified within 5 ppm mass measurement accuracy are summarized in Table 1. As a result, the total number of the identified tryptic fragments was 123 with

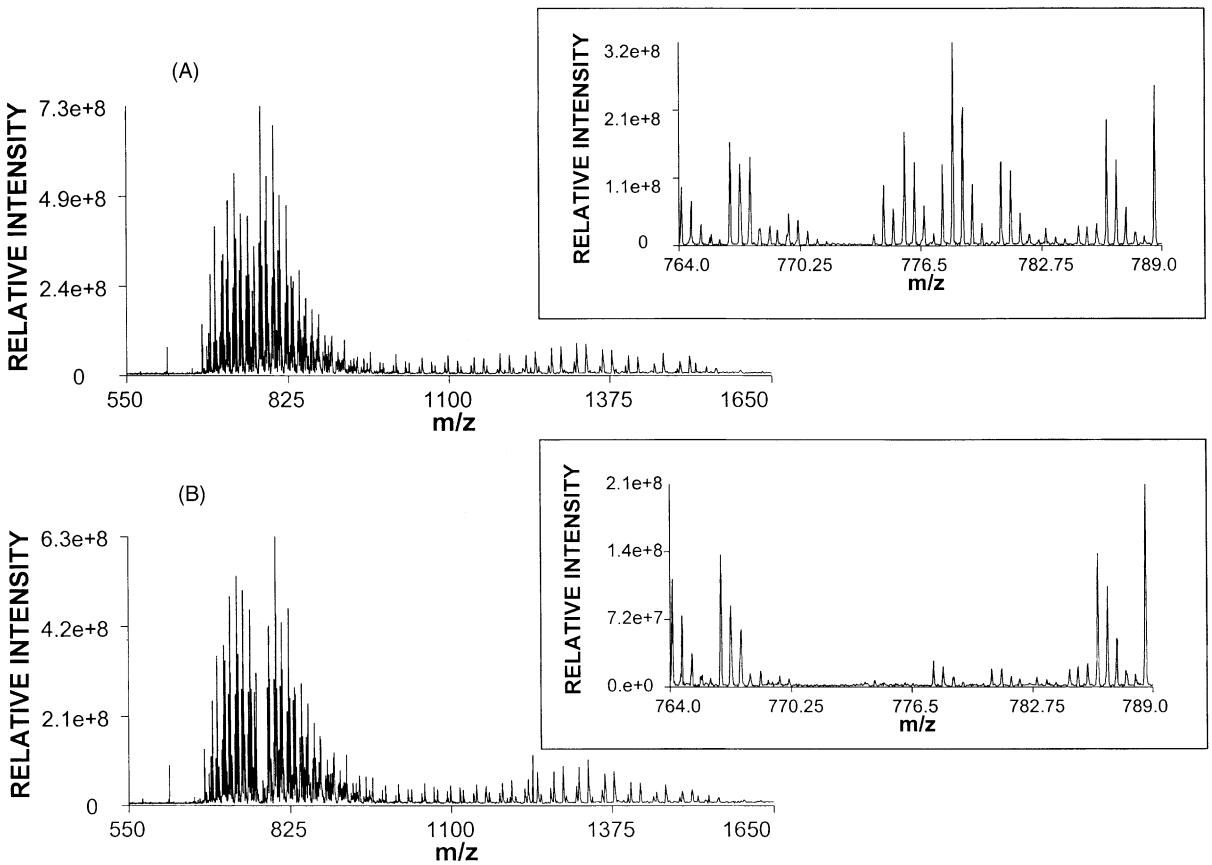

Fig. 5. Mass spectra obtained from a 10^{-7} M solution of (poly)ethylene glycol (MW = 1400 Da) in the "pseudo-trapping" mode. (A) Non-selective external ion accumulation. (B) Selective ion ejection mass spectrum acquired using parametric dipolar excitation. The excitation frequency and amplitude were 197 kHz and 300 mV_{p-p}, respectively.

82 being unique, providing 100% sequence coverage of the protein. Sixty unique tryptic fragments were detected using non-selective accumulation, while 22 (highlighted with bold italic font) were identified with selective accumulation. These results from a lower magnetic field instrument have good correlation with earlier reported results from our 11.5 T FTICR mass spectrometer [47]. In those experiments a five-fold more concentrated BSA tryptic digest was directly injected into the ESI source and acquired mass spectra were averaged over 100 scans. From the detected isotopic distributions, 86 could be ascribed to tryptic fragments of BSA on the basis of mass measurement errors of 10 ppm or less. Of these, 71 were within 2 ppm error limits corresponding to a complete amino acid sequence and an average error of 0.77 ppm. It should be mentioned, however, that in the case of more complex proteolytic digests (e.g., yeast) direct infusion experiments result in biased representation of the analyzed sample due to electrospray ionization suppression for less abundant and more acidic peptides, thus making LC/ESI/FTICR approach more attractive.

Fig. 7A shows a portion of the TIC chromatogram corresponding to a selected region of the mass spectra ($945 < m/z < 946$) acquired using the non-selective accumulation. The doubly charged peptide HPYFYAPELLYYANK (t20, 1887.92 Da) (Fig. 6A) was

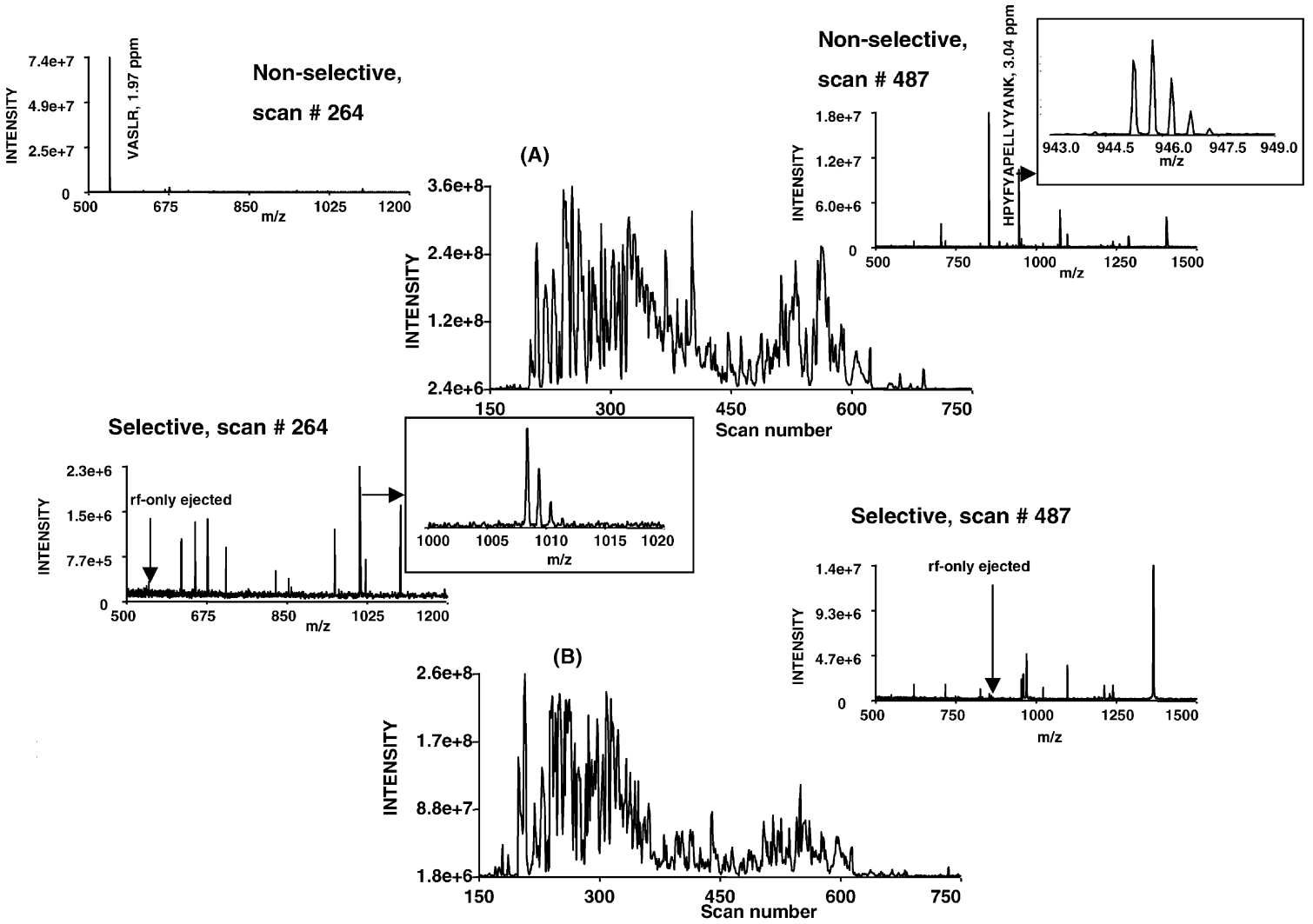

Fig. 6. The total ion current (TIC) chromatograms obtained from a 0.1 mg/mL bovine serum albumin digest acquired using data-dependent selective external ion accumulation (DREAMS). The experimental script for DREAMS is described in [29]. (A) The TIC (*m/z* 500–2000) obtained using the non-selective external ion accumulation. Accumulation time was 0.5 s followed by a 200 ms storage period. (B) The TIC (*m/z* ranging 500–2000) obtained using data-dependent selective ejection of the most abundant ion species prior to external accumulation. Accumulation time was 2 s followed by a 200 ms storage period. The insets demonstrate the mass spectra acquired during scans 264 and 487.

Table 1
The table of unique bovine serum albumin tryptic peptides identified within 5 ppm using LC/ESI/DREAMS/FTICR (Fig. 6)

Measured *m/z*	Calculated *m/z*	Fragments	Sequence	MMA (ppm)
544.3343	544.3333	t9	VASLR	1.977
571.3543	571.3554	t26,2	QRLR	2.7
657.3061	657.3082	t11	QEPER	3.194
702.3591	702.4024	t25	VLASSAR	5.476
718.4071	718.4092	t22	GACLLPK + H_2O	1.509
769.3578	769.36532	t45	NYQEAK + H_2O	1.349
846.4945	846.4963	t32,2	LSQKFPK	2.178
926.489	926.4861	t18	YLYEIAR	3.166
958.4363	958.42828	t12	NECFLSHK − H_2O	3.465
973.4534	973.4505	t4	DLGEEHFK	3.072
987.5637	987.56	t64,2	TPVSEKVTK	1.966
992.4062	992.39738	t54	QNCDQFEK − H_2O	3.806
1001.5779	*1001.5757*	*t78*	*LVVSTQTALA*	*2.278*
1005.441	1005.43238	t66	CCTESLVNR − H_2O	3.913
1010.4112	1010.4127	t54	QNCDQFEK	1.509
1013.6148	1013.612	t72	QTALVELLK	2.769
1014.4827	1014.4804	t42	SHCIAEVEK	2.328
1019.5867	1019.59102	t78	LVVSTQTALA + H_2O	0.477
1023.4439	1023.4477	t66	CCTESLVNR	3.779
1031.4779	1031.46978	t77	EACFAVEGPK − H_2O	3.287
1051.446	1051.4426	t61	CCTKPESER	4.215
1125.5824	1125.58652	t15,3	ADEKKFWGK + H_2O	0.538
1141.709	1141.707	t71,2	KQTALVELLK	1.781
1178.5426	1178.53418	t44,2	DVCKNYQEAK − H_2O	3.144
1180.6383	*1180.63862*	*t6*	*LVNELTEFAK + H_2O*	*3.788*
1192.5908	1192.5948	t1,2	DTHKSEIAHR	0.427
1248.6174	1248.6138	t3,2	FKDLGEEHFK	2.902
1304.7084	1304.7088	t53	HLVDEPQNLIK	0.299
1363.472	*1363.473*	*t10*	*ETYGDMADCCEK*	*0.727*
1387.5592	*1387.5635*	*t50*	*EYEATLEECCAK*	*3.143*
1398.6815	*1398.6853*	*t75*	*TVMENFVAFVDK*	*2.733*
1438.8105	1438.8044	t47,2	RHPEYAVSVLLR	4.288
1438.845	1438.83608	t30,3	ALKAWSVARLSQK − H_2O	2.167
1478.6204	*1478.60878*	*t51*	*DDPHACYSTVFDK*	*4.681*
1478.7915	1478.7881	t55	LGEYGFQNALIVR	2.334
1481.7931	1481.7911	t63,2	LCVLHEKTPVSEK	3.277
1494.8729	1494.86948	t24,4	EKVLASSARQRLR − H_2O	0.887
1521.9171	1521.92892	t72,2	QTALVELLKHKPK	4.709
1566.74	1566.7354	t46	DAFLGSFLYEYSR	2.978
1615.7383	1615.7412	t11,2	QEPERNECFLSHK	1.822
1633.7567	1633.75652	t11,2	QEPERNECFLSHK	2.962
1691.9362	1691.9345	t34,2	AEFVEVTKLVTDLTK	1.034
1717.7935	1717.79492	t49,2	LAKEYEATLEECCAK + H_2O	1.946
1719.793	1722.8365	t51,2	DDPHACYSTVFDKLK	0.249
1722.8351	*1722.8365*	*t46,2*	*DAFLGSFLYEYSRR*	*0.815*
1769.0331	1769.03582	t47,3	RHPEYAVSVLLRLAK	1.145
1804.8875	*1804.87698*	*t67*	*RPCFSALTPDETYVPK − H_2O*	*3.234*
1849.9129	1849.9138	t59,3	SLGKVGTRCCTKPESER	0.467
1868.0512	1886.0631	t25,4	VLASSARQRLRCASIQK	0.739
1887.9138	1887.9195	t20	HPYFYAPELLYYANK	3.042
1887.9821	1887.9876	t8,2	SLHTLFGDELCKVASLR	2.927
1898.9957	*1899.0002*	*t55,2*	*LGEYGFQNALIVRYTR*	*2.386*

Table 1 (*Continued*)

Measured *m/z*	Calculated *m/z*	Fragments	Sequence	MMA (ppm)
1941.8149	1941.8131	t36,2	VHKECCHGDLLECADDR	0.958
1941.9695	1941.9696	t2,3	SEIAHRFKDLGEEHFK	0.059
1943.9305	1943.92498	t14,2	LKPDPNTLCDEFKADEK − H_2O	0.371
1964.1014	*1964.10022*	*t29,4*	*FGERALKAWSVARLSQK − H_2O*	*3.044*
2044.0189	2044.0206	t19,2	RHPYFYAPELLYYANK	0.833
2086.92	2086.91138	t75,2	TVMENFVAFVDKCCAADDK	1.874
2382.1408	2382.13648	t43,2	DAIPENLPPLTADFAEDKDVCK	0.175
2434.2337	2434.2354	t5	GLVLIAFSQYLQQCPFDEHVK	0.698
2458.0916	*2458.10852*	*t36,3*	*VHKECCHGDLLECADDRADLAK + H_2O*	*4.997*
2483.1457	2483.1386	t11,3	QEPERNECFLSHKDDSPDLPK	2.888
2608.3043	2608.2994	t14,4	LKPDPNTLCDEFKADEKKFWGK	1.878
2694.2596	*2694.25148*	*t35,3*	*LVTDLTKVHKECCHGDLLECADDR − H_2O*	*1.248*
2755.5112	*2755.50128*	*t23,6*	*IETMREKVLASSARQRLRCASIQK*	*1.896*
2800.6529	2800.6537	t70,5	QIKKQTALVELLKHKPKATEEQLK	0.288
2951.4117	*2951.4221*	*t42,2*	*SHCIAEVEKDAIPENLPPLTADFAEDK*	*3.549*
2957.4477	2957.4327	t13,4	DDSPDLPKLKPDPNTLCDEFKADEKK	5.111
3301.6138	*3301.62902*	*t38,4*	*ADLAKYICDNQDTISSKLKECCDKPLLEK + H_2O*	*3.179*
3339.8571	*3339.85258*	*t25,7*	*VLASSARQRLRCASIQKFGERALKAWSVAR + H_2O*	*0.063*
3396.6066	3396.6216	t42,3	SHCIAEVEKDAIPENLPPLTADFAEDKDVCK	4.438
3488.77	*3488.77562*	*t17,4*	*FWGKYLYEIARRHPYFYAPELLYYANK + H_2O*	*0.243*
3488.7712	*3488.77562*	*t17,4*	*FWGKYLYEIARRHPYFYAPELLYYANK + H_2O*	*0.103*
3815.8941	*3815.89422*	*t64,4*	*TPVSEKVTKCCTESLVNRRPCFSALTPDETYVPK*	*1.23*
3828.6045	*3828.601*	*t10,4*	*ETYGDMADCCEKQEPERNECFLSHKDDSPDLPK*	*0.919*
3867.2145	*3867.2137*	*t30,7*	*ALKAWSVARLSQKFPKAEFVEVTKLVTDLTKVHK*	*0.22*
4010.2302	*4010.24022*	*t29,7*	*FGERALKAWSVARLSQKFPKAEFVEVTKLVTDLTK + H_2O*	*1.329*
4148.0643	*4148.05288*	*t44,5*	*DVCKNYQEAKDAFLGSFLYEYSRRHPEYAVSVLLR − H_2O*	*1.617*
4530.335	*4494.30678*	*t54,5*	*QNCDQFEKLGEYGFQNALIVRYTRKVPQVSTPTLVEVSR + H_2O*	*0.508*
4837.3451	*4837.34402*	*t35,6*	*LVTDLTKVHKECCHGDLLECADDRADLAKYICDNQDTISSKLK*	*1.217*
4839.4244	4839.4229	t1,5	DTHKSEIAHRFKDLGEEHFKGLVLIAFSQYLQQCPFDEHVK	0.309
7567.653	*7567.6298*	*t44,9*	*DVCKNYQEAKDAFLGSFLYEYSRRHPEYAVSVLLRLAKEY-*EATLEECCAKDDPHACYSTVFDKLK	*3.07*

The unique tryptic peptides detected with the selective accumulation sequence are highlighted in italics. In the fragments column the first index indicates the number of a tryptic fragment, while the second one shows the number of missed cleavages.

detected in five consecutive non-selective accumulation scans (scan numbers 487 through 491). Fig. 7B depicts the mass measurement accuracy as a function of the scan number for the LC peak in Fig. 7A. The experimental error was found to vary from −3.04 ppm (scan number 487) to 32.89 ppm (scan number 490), depending both on the total number of charges trapped in the FTICR cell and on the proximity of cyclotron frequencies of other detected ion species. An average error for HPYFYAPELLYYANK peptide over its elution time was 22.7 ppm.

Several conclusions can be drawn from the results shown in Table 1 and Fig. 7A and B. First, the elution time of higher abundant peaks was typically ∼20 s, covering several mass spectrum acquisitions (e.g., each of five 0.5 s non-selective accumulation scans was immediately followed by a 2 s selective accumulation scan in Fig. 7A). Therefore, the majority of the unique tryptic fragments detected during the selective accumulation scans resulted from the dynamic range enhancement of the accumulation quadrupole due to selective ejection of the most abundant ion species prior to ion accumulation for an extended period. Compared to the conventional capillary LC/ESI/non-selective external ion accumulation/FTICR (60 unique tryptic fragments), capillary LC/ESI/DREAMS/FTICR increased the number of identified peptides by ∼35% (additional 22 unique

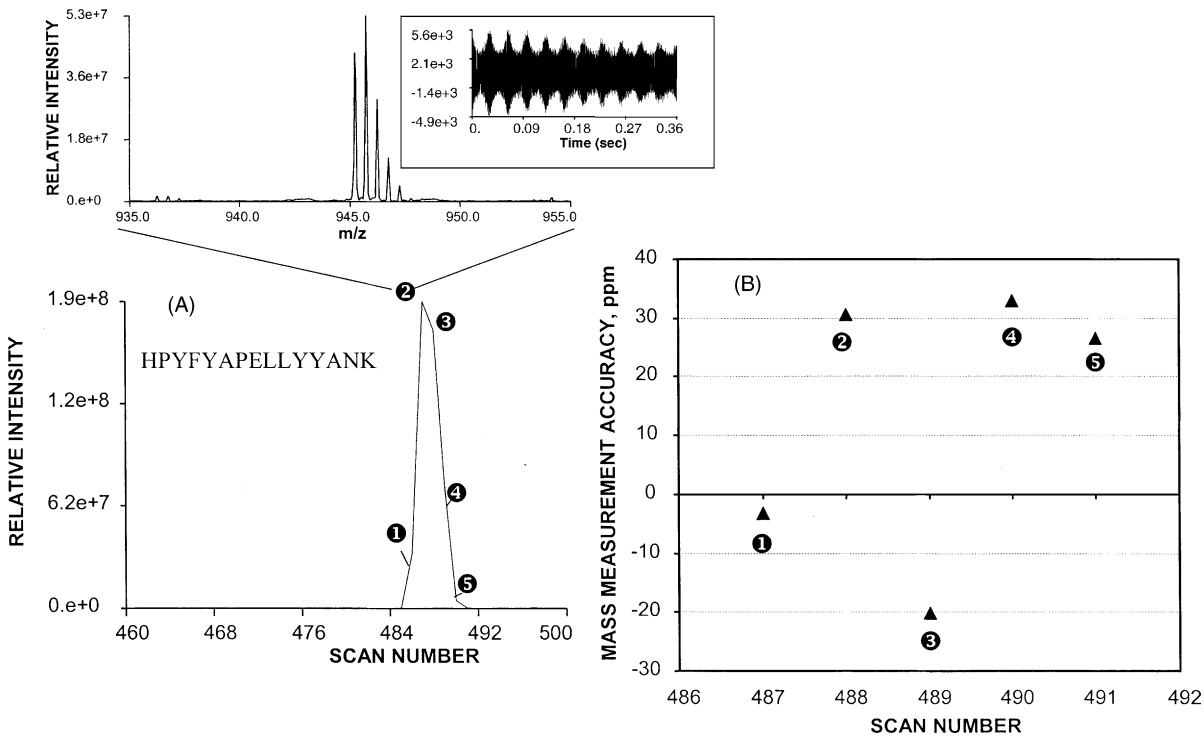

Fig. 7. (A) A portion of the total ion current (TIC) chromatogram corresponding to a selected region of the mass spectra ($945 < m/z < 946$) acquired using the non-selective accumulation. The inset demonstrates the mass spectrum corresponding to this m/z region. (B) Mass measurement error (uncorrected) in identification of HPYFYAPELLYYANK tryptic peptide as a function of the non-selective accumulation scan number.

fragments), consistent with our earlier observations [29]. Second, the space charge induced effect upon ion cyclotron frequencies (Fig. 7B) requires correction both for the number of ions trapped in the FTICR cell (global space charge effect) and for interaction between ion clouds at close cyclotron frequencies (local space charge effect). Both global and local space charge effects can be corrected for by introduction of an external calibrant into the FTICR cell and performing calibration using this sample [48,49]. To avoid interference with the DREAMS selective ejection, the calibrant can be directly injected into the FTICR cell from the side opposite to the ESI source using alternative ionization technique (e.g., laser desorption or by otherwise controlling ion injection from a secondary ion source) or through the dual ion funnel interface. Following data acquisition the cyclotron frequencies of calibrant ion peaks from each individual scan (drifting due to the aforementioned space charge effects in the FTICR cell) are then calculated using the global calibration function (i.e., from the calibration equation used for a particular LC run) and each individual spectrum is then recalibrated based on the calibrant ion frequencies.

To summarize, correction for the fringing rf-fields in the selection quadrupole improved mass resolution for ion ejection by a factor of 3 as compared to that of a conventional quadrupole and increased the efficiency of the DREAMS approach in identification of tryptic peptides from LC separations of proteolytic digests. It should be noted that higher mass resolution could be achieved by trapping a small constant number of ions in the segmented selection quadrupole operating at higher Mathieu parameter

($q \sim 0.7$). These ions would then be ejected from the selection quadrupole for extended storage periods by applying lower-amplitude resonant dipolar excitation. In this case frequency drift for secular excitation would be less than 1%. However, this approach would result in a reduced duty cycle and, therefore, less efficient detection of lower abundance peptides. In addition, since q is an m/z-dependent parameter, mass resolution would decrease with an increase in m/z. We believe that DREAMS ion ejection in the "pseudo-trapping" mode is an attractive alternative for proteomic applications providing a resolution of ~100 for abundant ion ejection across the mass spectrum while maintaining higher duty cycle. When combined with the automated gain control capability (i.e., data-dependent adjustment of ion accumulation time based on TIC measurements) being developed at our laboratory, DREAMS FTICR is expected to significantly enhance proteomic studies.

Acknowledgements

The authors are grateful to Ron Moore for packing the LC columns. Portions of this research were supported by the office of Biological and Environmental Research, US Department of Energy, and the National Cancer Institute under Grant CA81654. Pacific Northwest National Laboratory is a multiprogram national laboratory operated by Battelle Memorial Institute for the US Department of Energy under contract DE-AC06-76RLO 1830.

References

[1] J.F. Banks, J.P. Quinn, C.M. Whitehouse, Anal. Chem. 66 (1994) 3688.
[2] G. Neubauer, R.J. Anderegg, Anal. Chem. 66 (1994) 1056.
[3] S.K. Chowdhury, J. Eshraghi, H. Wolfe, D. Forde, A.G. Hlavac, D. Johnston, Anal. Chem. 67 (1995) 390.
[4] J.R. Yates, A.L. McCormack, A.J. Link, D. Schieltz, J. Eng, L. Hays, Analyst 121 (1996) R65.
[5] P.A. DeAgostino, J.R. Hancock, L.R. Provost, J. Chromatogr. A 767 (1997) 77.
[6] K.L. Stone, R. DeAngelis, M. LoPresti, J. Jones, V.V. Papov, K.R. Williams, Electrophoresis 19 (1998) 1046.
[7] Y. Oda, K. Huang, F.R. Cross, D. Cowburn, B.T. Chait, Proc. Natl. Acad. Sci. U.S.A. 96 (1999) 6591.
[8] J.R. Yates, E. Carmack, L. Hays, A.J. Link, J.K. Eng, Math. Mol. Biol. 112 (1999) 553.
[9] S.P. Gygi, B. Rist, S.A. Gerber, F. Turecek, M.H. Gelb, R. Aebersold, Nat. Biotechnol. 17 (1999) 994.
[10] J.R. Yates, Trends Genet. 17 (2000) 81.
[11] R.D. Smith, Int. J. Mass Spectrom. 200 (2000) 509.
[12] J. Godovac-Zimmerman, L. Brown, Mass Spectrom. Rev. 20 (2000) 1.
[13] R. Aebersold, D.R. Goodlett, Chem. Rev. 101 (2001) 269.
[14] G.W. Stockton, J.T. Meek, W.G. Millen, R.S. Wayne, in: B. Asamoto (Ed.), FT-ICR/MS: Analytical Applications of Fourier Transfrom Ion Cyclotron Resonance Mass Spetrometry, New York, VCH, 1991, p. 235.
[15] M.B. Comisarow, A.G. Marshall, Chem. Phys. Lett. 25 (1974) 282.
[16] A.G. Marshall, Int. J. Mass Spectrom. 200 (2000) 331.
[17] M.E. Belov, E.N. Nikolaev, G.A. Anderson, H.R. Udseth, T.P. Conrads, T.D. Veenstra, C.D. Masselon, M.V. Gorshkov, R.D. Smith, Anal. Chem. 73 (2001) 253.
[18] Y. Shen, R. Zhao, M.E. Belov, T.P. Conrads, G.A. Anderson, K. Tang, L. Pasa-Tolic, T.D. Veenstra, M.S. Lipton, R.D. Smith, Anal. Chem. 73 (2001) 1766.
[19] T.P. Conrads, K. Alving, T.D. Veenstra, M.E. Belov, G.A. Anderson, D.J. Anderson, L. Pasa-Tolic, W.B. Chrisler, B.D. Trall, R.D. Smith, Anal. Chem. 73 (2001) 2132.
[20] Y. Shen, N. Tolic, R. Zao, L. Pasa-Tolic, L. Li, S.J. Berger, R. Harkewicz, G.A. Anderson, M.E. Belov, R.D. Smith, Anal. Chem. 73 (2001) 3011.
[21] M.W. Senko, C.L. Hendrikson, M.R. Emmett, S.D.-H. Shi, A.G. Marshall, J. Am. Soc. Mass Spectrom. 8 (1997) 970.
[22] R. Mciver, US Patent 4,535,235 (1985).
[23] S.C. Beu, D.A. Laude Jr., Int. J. Mass Spetrom. Ion Proc. 104 (1991) 109.
[24] Y. Wang, S.D.-H. Shi, C.L. Hendrickson, A.G. Marshall, Int. J. Mass Spectrom. 198 (2000) 113.
[25] M.E. Belov, E.N. Nikolaev, G.A. Anderson, K.J. Auberry, R. Harkewicz, R.D. Smith, J. Am. Soc. Mass Spectrom. 12 (2001) 38.
[26] W. Paul, H.P. Reinhard, U. von Zahn, Z. Physik 152 (1958) 143.
[27] D.J. Douglas, US Patent 5,179,278 (1993).
[28] J.M. Campbell, B.A. Collings, D.J. Douglas, Rapid Commun. Mass Spectrom. 12 (1998) 1463.
[29] M.E. Belov, G.A. Anderson, N.H. Angell, Y. Shen, N. Tolic, R.D. Smith, Anal. Chem. 73 (2001) 1552.
[30] B. Cha, M. Blades, D.J. Douglas, Anal. Chem. 72 (2000) 5647.
[31] P.H. Dawson (Ed.), Quadrupole Mass Spectrometry and Its Applications, Elsevier, New York, 1976.
[32] H.G. Dehmelt, Adv. Atom. Mol. Phys. 3 (1967) 53.
[33] W.M. Brubaker, Advances in Mass Spectrom, Vol. 4, Elsevier, Amsterdam, 1968.
[34] P.H. Dawson, Int. J. Mass Spectrom. Ion Phys. 6 (1971) 33.
[35] W.L. Fite, Rev. Sci. Instrum. 47 (1976) 326.

[36] M.E. Belov, E.N. Nikolaev, R. Harkewicz, C.D. Masselon, K. Alving, R.D. Smith, Int. J. Mass Spectrom. 208 (2001) 205.
[37] M.E. Belov, M.V. Gorshkov, G.A. Anderson, H.R. Udseth, R.D. Smith, Anal. Chem. 72 (2000) 2271.
[38] P. Kofel, M. Allemann, H. Kellerhals, K.P. Wanczek, Int. J. Mass Spectrom. Ion Proc. 65 (1985) 97.
[39] R.T. McIver Jr., R.L. Hunter, W.D. Bowers, Int. J. Mass Spectrom. Ion Proc. 64 (1985) 67.
[40] J.M. Alford, P.E. Williams, D.J. Trevor, R.E. Smalley, Int. J. Mass Spectrom. Ion Proc. 72 (1986) 33.
[41] D.M. Eades, J.V. Johnson, R.A. Yost, J. Am. Soc. Mass Spectrom. 4 (1993) 917.
[42] N. Bogoliubov, J. Mitropolsky, Asymptotic Methods in the Theory of Non-Linear Oscillations (in Russian), Moscow, 1958.
[43] Y.A. Mitropol'kii, Problems of the Asymptotic Theory of Non-Stationary Vibrations, Daniel Davey, New York, 1965.
[44] N. Minorsky, Non-Linear Oscillations, Van Nostrand, Princeton, 1962.
[45] A.A. Makarov, Anal. Chem. 68 (1996) 4257.
[46] S. Sevugarajan, A.G. Menon, Int. J. Mass Spectrom. 197 (2000) 263.
[47] J.E. Bruce, G.A. Anderson, J. Wen, R. Harkewicz, R.D. Smith, Anal. Chem. 71 (1999) 2595.
[48] E.F. Gordon, D.C. Muddiman, Rapid. Commun. Mass Spectrom. 13 (1999) 164.
[49] J.W. Flora, J.C. Hannis, D.C. Muddiman, Anal. Chem. 73 (2001) 1247.